Experimental evidence for rock layering development by pressure solution

Jean-Pierre Gratier[1,2], Catherine Noiriel[3], and François Renard[1,2,4]
[1]ISTerre, Université Grenoble Alpes, 38041 Grenoble Cedex 9, France
[2]ISTerre, CNRS, 38041 Grenoble Cedex 9, France
[3]Géosciences Environnement Toulouse, Observatoire Midi-Pyrénées, Université Paul Sabatier, CNRS, IRD, 31400 Toulouse, France
[4]Physics of Geological Processes, Department of Geosciences, University of Oslo, 0316 Oslo, Norway

ABSTRACT

Natural deformation of rocks is commonly associated with development of mineralogical layering, leading to irreversible transformations of their microstructure. The mechanisms of such chemical differentiation processes during diagenesis, tectonics, metamorphism, or fault differentiation remain poorly understood, as they are difficult to reproduce experimentally due to the very slow kinetics involved. This paper shows that development of differentiated layering, similar to that observed in natural deformation, is stress driven and can be obtained from indenter experiments. Samples of (1) gypsum plaster mixed with clay, and (2) natural diatomite loosely interbedded with volcanic ash, saturated with aqueous solutions in equilibrium, were subjected to loading for several months at 40 °C and 150 °C, respectively. X-ray microtomography and scanning electron microscopy observations show that layering develops by a self-organized pressure solution process. Stress-driven dissolution of the soluble minerals (either gypsum or silica) is initiated in the areas initially richer in insoluble species (clay or volcanic ash), as diffusive mass transfer along the interface between soluble and insoluble minerals is much faster than along the healed boundaries of the soluble minerals. The passive concentration of the insoluble minerals amplifies the dissolution along layers oriented perpendicularly to the maximum compressive stress. Conversely, in areas with an initial low content of insoluble minerals and clustered soluble minerals, dissolution is slower. Consequently, these areas are less deformed; they host the re-deposition of the soluble species and act as rigid objects that concentrate both stress and dissolution near their boundaries, thus amplifying the differentiation and the development of layered microstructures.

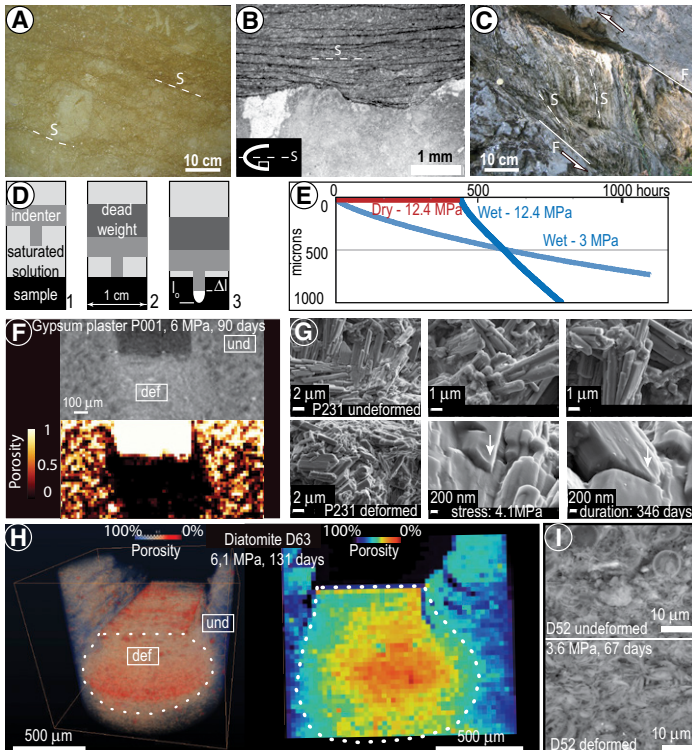

Figure 1. A–C: Various types of layering development resulting from natural deformation in carbonate rocks: diagenetic layering (A); dissolution cleavage in fold (B); and dissolution cleavage in fault gouge (C). S—differentiated layer; F—fault. D: Experimental set-up. Δl is indenter displacement; l_o is the distance between the top of the sample and the base of the deformed zone (white zone in H). E: Graph of displacement versus time for gypsum plaster indenting for dry (red) and wet (blue) samples. F,H: X-ray micro-computed tomography images of deformed gypsum plaster (F) (two-dimensional cross-section) and diatomite (H) (three-dimensional rendering and two-dimensional cross-section), with gray and color level coding indicating X-ray absorption and the porosity of the materials, respectively. und—undeformed; def—deformed. G,I: Grain-scale scanning electron microscope observations in undeformed (top panels) and deformed (bottom panels) gypsum plaster (G) and diatomite (I) samples.

INTRODUCTION

Natural deformation of rocks is commonly associated with chemical differentiation processes at all scales, from intra-crystalline oscillatory zoning to basin compartmentation (Ortoleva, 1993). The development of differentiated mineral layering is associated with deformation of polycrystalline rocks, such as the amplification of sedimentary oscillations during diagenetic processes (Fig. 1A), the development of foliated cleavage during tectonic (Fig. 1B) and metamorphic processes (Wintsch et al., 2005), and the differentiation process in fault gouges (Fig. 1C). It is generally assumed that differentiated layering develops by amplification of initial compositional or textural heterogeneities (Cobbold, 1977; De Vore, 1969; Robin, 1979) related to a self-organized process (Ortoleva, 1993). According to this idea, an irreversible self-organized change in the initial rock texture and composition is postulated to occur through a positive feedback between mechanochemical reactions and mass transport under differential stress. Various property changes have been proposed theoretically, which could lead to critical feedback processes such as changes in porosity (Merino et al., 1983), mineral composition (Dewers and Ortoleva, 1989; Putnis, 2002; Wintsch et al., 2005), material strength (Montesi, 2007; Robin, 1979), and permeability (Heap et al., 2014). Strain localization has been produced with very-large-shear experiments ($\gamma > 4$), (Barnhoorn et al., 2005). However, rock layering development associated with compaction as in natural examples (Fig. 1) had yet to be reproduced experimentally. We thought that this could be because it is controlled by stress-driven processes, which are very slow (Renard and Ortoleva, 1997; Wheeler, 2014). We overcame this obstacle by performing long-term indenter experiments, over several months, and by using material with high initial porosity and solid-fluid associations leading to high solubility for at least one mineral.

METHODS

The experiments were performed using the indenter technique developed for pressure solution creep studies (Gratier et al., 2013). Table DR1

in the GSA Data Repository[1] summarizes the experimental conditions for the deformed samples that are discussed here. Other experiments, performed to study reproducibility, lead to the same observations (see the Data Repository). Indenters of various shapes (either cylindrical or rectangular) and sizes were mounted under a free-moving piston. The indenters were placed in contact with cylindrical samples, either gypsum plaster or diatomite, previously saturated with an aqueous solution at chemical equilibrium with the samples under the experimental conditions. A dead weight fixed on the piston sets the vertical stress. A schematic view of the experimental apparatus is shown in Figure 1D.

For experiments with gypsum, the samples were produced from pure $CaSO_4$, 0.5 H_2O powder (bassanite) mixed with 10% clay (illite) and water (see the Data Repository). After drying, initial porosity is ~53%. A layer of liquid paraffin was poured around the indenter after sample saturation in order to prevent evaporation. The whole setup was placed in an oven at 40 °C and under atmospheric pressure for several months. The vertical displacement of the indenter was recorded at a sampling rate of three measurements per hour by a set of three high-resolution displacement sensors (linear encoders, Solartron interferometer, with less than 0.5 µm accuracy) fixed every 120° around the indenter (Gratier et al., 2014).

For experiments with diatomite, the indenting was performed perpendicular to the preexisting layering. Diatomite was extracted from a quarry in Saint-Bauzile (France). The formation was deposited in a lake of volcanic origin ~7.5 m.y. ago. The rock is made of an accumulation of silica fossil tests of diatoms more or less interlayered with volcanic material, including glass shards, silicates, and alumino-silicates (Pastre et al., 2004). Initial porosity is ~68%. For the experiments, the indenter device was kept inside a pressure vessel for several months at constant temperature (150 °C) and fluid pressure (20 MPa). The solution was saturated in a NaOH 1 M solution in order to increase the solubility of silica by ~20× compared to that for pure water (Gratier et al., 2009). The final displacement of the indenter was measured by optical means at the end of the experiment.

The deformed samples were analyzed using two types of technique:

(1) Three-dimensional X-ray micro-computed tomography (XMT) was acquired, with a voxel resolution of 5 µm for gypsum plaster and 0.37 µm for diatomite. Imagery was performed at University of Bordeaux and European Radiation Synchrotron Facility (ID19 beamline), respectively. The data were processed using the software AvizoFire to map porosity distribution. The porosity was calculated based on the gray-level distribution within the XMT data set, with the porosity set to the initial porosity of the sample in the undeformed areas.

(2) Two-dimensional observations and chemical mapping were performed on sample cross-sections using a field emission scanning electron microscope (FE-SEM, ZEISS Ultra 55) coupled with electron dispersive spectroscopy (EDS) for microanalyses (silicon drift detector [SDD], Bruker AXS–30 mm^2).

OBSERVATIONS AND ANALYSES

Changes in Porosity

Gypsum Plaster Indenting

The indenter displacement variation with time (Fig. 1E) shows the progressive deformation of the wet sample. Under similar conditions, no displacement is observed in the dry condition (Fig. 1E). When adding a saturated solution the displacement is seen immediately. Figure 1F (top) illustrates the compaction process below the indenter, with a drastic change in porosity from an initial 53% to nearly 0% (Fig. 1F, bottom). This densification accommodates a deformation ($\Delta l/l_o$) of 0.53, which is in good agreement with the vertical compaction of the sample related to the displacement of the indenter (with Δl = 500 µm and l_o = 1000 µm; see Fig. 1H). The SEM images show the change in structure from the undeformed areas (laterally away from the indenter) to the deformed areas (i.e., below the indenter). In the undeformed state, gypsum crystals are oriented in all directions with large voids between the crystals (Fig. 1G, top). In the deformed compacted state, the crystals are more densely packed, with some evidence of crystals indenting (Fig. 1G, bottom).

Diatomite Indenting

Similar behavior is observed for the diatomite samples. The porosity, initially equal to 68%, is drastically reduced under the indenter, to nearly 45% on average, with a local maximum reduction down to 27% (Fig. 1H). The porosity reduction corresponds to a deformation ($\Delta l/l_o$) of 0.42, which is also in good agreement with the vertical compaction of the sample related to the displacement of the indenter (with Δl = 700 µm and l_o = 1600 µm) (see Fig. 1H). SEM observations reveal that the deformed area below the indenter is associated with a sub-horizontal tangle of silica fossil tests (Fig. 1I, bottom), whereas some of the tests had been quite randomly oriented during deposition and remained undeformed during natural compaction of the rock (Fig. 1I, top).

Chemical Differentiation

Gypsum Plaster Indenting

Elemental map distribution (Fig. 2) shows a clear variation in the spatial distribution of the elements characteristic of the behavior of the various minerals within the samples: calcium and silicon maps characterize the spatial distribution of gypsum and illite, respectively. In the initial undeformed state, i.e., laterally away from the indenter (Fig. 2B), the illite that had been added to the gypsum plaster preparation is randomly distributed. Conversely, below the indenter, a layering phenomenon developed (underlined by dotted lines in Fig. 2), corresponding to the concentration of illite in thin differentiated layers. In more detail, almond-shaped areas can be distinguished with a low illite content, which are emphasized by illite-rich arched layers (Figs. 2C, 2D, and 2F). At higher magnification (Fig. 2E), the transition between illite-rich and illite-poor areas is sharp and less than a micrometer wide.

Diatomite Indenting

For diatomite (Fig. 3), the contrast between the behavior of the silica fossil tests and that of other minerals during deformation is best seen in Al element distribution maps, because Al is present in most of the minor minerals found in the rock, i.e., clays, biotite, sanidine, and augite (Figs. 3B–3D). Sedimentary layering (underlined by dotted lines in Fig. 3) already existed before compaction and was deformed and folded under the indenter. However, the Al distribution immediately below the indenter shows two wide layers of high Al content corresponding to differentiated layering (Figs. 3B–3D). Such high-Al-content layers are limited to the zone of influence of the indenter and do not extend laterally away from the indenter. As a consequence, they result from a differentiated layering process that also occurs within the diatomite, as for the gypsum plaster.

DISCUSSION AND CONCLUSIONS

Observations by XMT and SEM-EDS chemical maps reveal that two processes occurred simultaneously: (1) compaction below the indenter, which leads to a drastic reduction in porosity, and (2) chemical differentiation, during which the less soluble minerals (i.e., clays in gypsum plaster and volcanic ash in diatomite) concentrate along layers. Two factors must work together to obtain mineral segregation into localized layers of insoluble minerals that bound zones with a higher content of soluble minerals: (1) kinetics of chemical reactions, which control the rate of the

[1]GSA Data Repository item 2015293, details on the methodology, SEM-EDS images of another deformed sample, and various aspects of tectonic layering, is available online at www.geosociety.org/pubs/ft2015.htm, or on request from editing@geosociety.org or Documents Secretary, GSA, P.O. Box 9140, Boulder, CO 80301, USA.

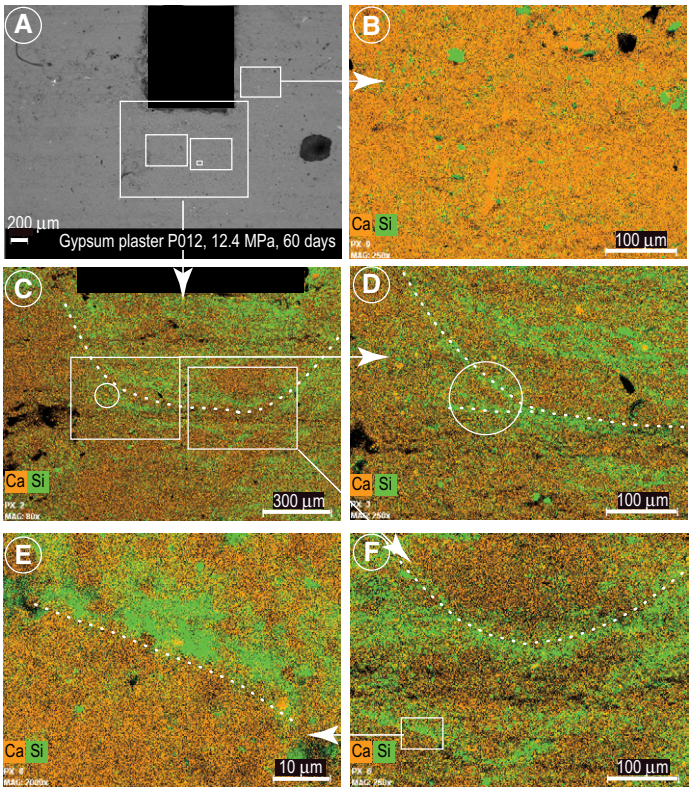

Figure 2. Scanning electron microscope–energy dispersive X-ray spectroscopy (SEM-EDS) images of gypsum plaster sample showing distribution map of soluble (gypsum = Ca, orange) and insoluble (illite = Si, green) species around indenter (black rectangle in A). From initial random distribution of illite (B), indenting leads to differentiated layering associated with passive concentration of illite, related to stress-driven dissolution of gypsum. Map distributions are given at various scales with location of images at larger magnifications (B–F) shown as white boxes. Black areas correspond to voids.

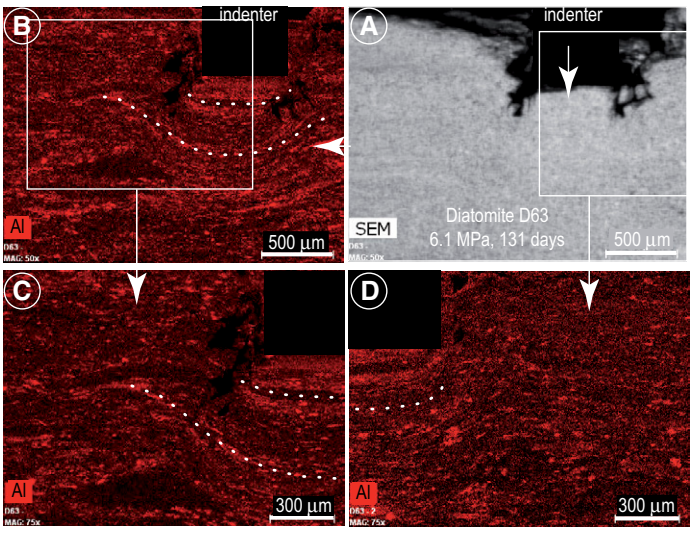

Figure 3. Scanning electron microscope–energy dispersive X-ray spectroscopy (SEM-EDS) images of diatomite sample showing distribution map of insoluble volcanic material (Al, red). Structure is initially slightly layered as a result of episodic volcanic ash deposition alternating with diatom development. Differentiated layering is amplified below indenter as shown by high concentration of Al that does not correspond to laterally away initial composition of the layer. Map distributions are given at various scales with location of images at larger magnifications (B–D) shown as white boxes.

process, and (2) thermodynamics of stress concentration, which drives the dissolution.

The kinetic effect arises from the fact that dissolution at the contact between soluble and insoluble minerals is most often faster than dissolution between two soluble neighboring minerals. The catalytic role of phyllosilicates has been observed both in nature (Heald, 1955) and in experiments (Meyer et al., 2006; Renard et al., 2001). More generally, diffusive mass transfer along the interface between soluble/insoluble minerals is much faster than along the healed boundaries of the soluble minerals, as shown in experiments (Hickman and Evans, 1991; van Noort et al., 2008) and in nature (Gratier et al., 2013). The explanation is that the contact between two soluble minerals is likely to become healed whereas the fluid phase trapped under stress at the interface between soluble and insoluble minerals is more continuous (Fig. 4, inset i). The more continuous and thicker the fluid phase, the faster the kinetics of diffusion is along the dissolution contact. This effect leads to a self-organized positive feedback: the higher the insoluble content in a particular area, the faster the kinetics, then the higher the dissolution of the soluble species in this particular area, which leads to the passive concentration of insoluble species that in turn accelerates the dissolution, and so on. It was not possible to identify the redeposited part of the dissolved species as it probably occurred on the free faces of the gypsum crystals or the diatom fragments. Re-deposition must have occurred very near the dissolution sites (Fig. 4) as there is no visible evidence of a porosity change away from the areas that have been compacted.

A stress concentration effect is coupled with the kinetic effect. The passive concentration of the insoluble species leads to local weakening of the preferred dissolution zone, which induces stress concentration at its boundary (Cosgrove, 1976). This effect explains the propagation of the localized dissolution in a plane perpendicular to the maximum compressive stress direction (Fig. 4, inset ii). This mechanism has been conceptualized through an anti-crack propagation process (Aharonov and Katsman, 2009; Fletcher and Pollard, 1981). The progressive mineral concentration may reach a point where almost 100% of insoluble species are concentrated along a differentiated layer (Fig. 2). At this stage, dissolution continues at the boundaries of the layer rich in insoluble species. Conversely, in the areas that contain initially a low content of insoluble species and clustered soluble minerals, dissolution remains more difficult, and re-deposition can

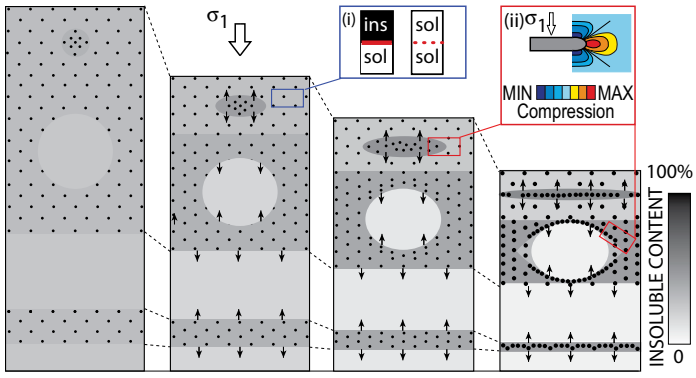

Figure 4. Conceptual model of self-organized process leading to differentiated layering in compacted zone: insoluble (ins) species are dark, soluble (sol) species are white , shades of gray correspond to various soluble and insoluble contents as shown by the color bar: the higher the content of insoluble species, the faster the dissolution of neighboring soluble species. Thin arrows indicate diffusive mass transfer. Inset i shows how the trapped fluid phase (in red) is more continuous between soluble-insoluble grain contacts than between soluble-soluble contacts, which are most often healed. Inset ii shows location of zone of maximum mean compressive stress (red) that leads to propagation of differentiated layer perpendicular to maximum compressive stress component (σ_1) from relatively weak insoluble stacking zone (gray).

occur on the free faces of the soluble species. Consequently these areas act as relatively strong and rigid domains that concentrate the stress around them and therefore dissolution near their boundaries (Fig. 4, right), thus amplifying the chemical differentiation.

Layering development modifies both the rheological and the transfer properties of rocks: a widespread strain localization process takes place in the upper crust when a reactive fluid phase is present (Gratier et al., 2013), complementary to other strain localization processes in the lithosphere (Montesi, 2007).

In conclusion, a crucial parameter involved in the self-organized mineralogical differentiation by pressure solution is the mixing of mineral species with highly contrasting solubilities. Another general requirement is the presence of a fluid phase that is a solvent for at least one of the minerals forming the rock. This is the case for the examples of diagenetic and tectonic layering and fault gouge differentiation (Fig. 1). In such cases, phyllosilicates and other insoluble species play the same role as in experiments (black minerals in Fig. 4), whereas calcite, quartz, feldspar, gypsum, and halite are the most common natural soluble species (white minerals in Fig. 4). Determining which parameters fix the width of the stress-driven layers remains a challenge (see the Data Repository). According to our interpretation, the modeling of chemical and compositional changes during natural deformation must be rooted in the stress-driven dissolution and transport properties of the various minerals forming the rocks, and in the change in their rheological and transfer properties. The change in strength can be taken into account by a weakening factor in the dissolution zone (Cosgrove, 1976) and a strengthening factor in the deposition zone (Gratier et al., 2013). The change in kinetics is controlled by the critical parameters of pressure solution (Bos and Spiers, 2002; Gratier et al., 2013; Rutter, 1976), which mainly depends on: (1) the solubility of the solid in solution, (2) the thickness and diffusion properties of the fluid phase trapped under stress between the grain contacts (emphasizing the activating effect of fluid phase continuity), (3) the stress driving force (the difference between normal stress on the dissolution surfaces and fluid pressure in the deposition area), and (4) the mean size of the grain contacts under stress (the inversely proportional relationship of which emphasizes the activating effect of high porosity).

ACKNOWLEDGMENTS

We thank J. Wheeler and M. Heap for their comments that helped to improve the manuscript, and R. Guiguet, B. Vial, and D. Olive for the help with the experiments. This study was supported by the Institut National des Sciences de l'Univers, the OSUG@2010 LabEx, the NEEDS CNRS, and the FISIC ANR programs.

REFERENCES CITED

Aharonov, E., and Katsman, R., 2009, Interaction between pressure solution and clays in stylolite development: Insights from modeling: American Journal of Science, v. 309, p. 607–632, doi:10.2475/07.2009.04.

Barnhoorn, A., Bystricky, M., Kunze, K., Burlini, L., and Burg, J.P., 2005, Strain localisation in bimineralic rocks: Experimental deformation of synthetic calcite-anhydrite aggregates: Earth and Planetary Science Letters, v. 240, p. 748–763, doi:10.1016/j.epsl.2005.09.014.

Bos, B., and Spiers, C.J., 2002, Frictional-viscous flow of phyllosilicate-bearing fault rock: Microphysical model and implications for crustal strength profiles: Journal of Geophysical Research, v. 107, doi:10.1029/2001JB000301.

Cobbold, P.R., 1977, Description and origin of banded deformation structures: Canadian Journal of Earth Sciences, v. 14, p. 2510–2523, doi:10.1139/e77-217.

Cosgrove, J.W., 1976, The formation of crenulation cleavage: Journal of the Geological Society, v. 132, p. 155–178, doi:10.1144/gsjgs.132.2.0155.

De Vore, G., 1969, Preferred mineral distributions of polymineralic rocks related to non-hydrostatic stresses as expressions of mechanical equilibria: The Journal of Geology, v. 77, p. 26–38, doi:10.1086/627406.

Dewers, T., and Ortoleva, P., 1989, Self-organization of mineralization patterns in metamorphic rocks through mechanochemical coupling: Journal of Physical Chemistry, v. 93, p. 2842–2848, doi:10.1021/j100344a028.

Fletcher, R.C., and Pollard, D.D., 1981, Anticrack model for pressure solution surfaces: Geology, v. 9, p. 419–424, doi:10.1130/0091-7613(1981)9<419:AMFPSS>2.0.CO;2.

Gratier, J.-P., Guiguet, R., Renard, F., Jenatton, L., and Bernard, D., 2009, A pressure solution creep law for quartz from indentation experiments: Journal of Geophysical Research, v. 114, B03403, doi:10.1029/2008JB005652.

Gratier, J.-P., Dysthe, D.K., and Renard, F., 2013, The role of pressure solution creep in the ductility of the Earth's upper crust: Advances in Geophysics, v. 54, p. 47–179, doi:10.1016/B978-0-12-380940-7.00002-0.

Gratier, J.-P., Renard, F., and Vial, B., 2014, Postseismic pressure solution creep: Evidence and time-dependent change from dynamic indenting experiments: Journal of Geophysical Research, v. 119, p. 2764–2779, doi:10.1002/2013JB010768.

Heald, M.T., 1955, Stylolites in sandstones: The Journal of Geology, v. 63, p. 101–114, doi:10.1086/626237.

Heap, M.J., Baud, P., Reuschle, T., and Meredith, P.G., 2014, Stylolites in limestones: Barriers to fluid flow?: Geology, v. 42, p. 51–54, doi:10.1130/G34900.1.

Hickman, S.H., and Evans, B., 1991, Experimental pressure solution in halite: The effect of grain/interphase boundary structure: Journal of the Geological Society, v. 148, p. 549–560, doi:10.1144/gsjgs.148.3.0549.

Merino, E., Ortoleva, P., and Strickholm, P., 1983, Generation of evenly spaced pressure solution seams during late diagenesis: A kinetics theory: Contributions to Mineralogy and Petrology, v. 82, p. 360–370, doi:10.1007/BF00399713.

Meyer, E.E., Greene, G.W., Alcantar, N.A., Israelachvili, J.N., and Boles, J.R., 2006, Experimental investigation of the dissolution of quartz by a muscovite mica surface: Implications for pressure solution: Journal of Geophysical Research, v. 111, B08202, doi:10.1029/2005JB004010.

Montesi, L.G.J., 2007, A constitutive model for layer development in shear zones near the brittle-ductile transition: Geophysical Research Letters, v. 34, L08307, doi:10.1029/2007GL029250.

Ortoleva, P., 1993, Self-organization and non-linear dynamics in sedimentary basins: Philosophical Transactions of the Royal Society of London A, v. 344, p. 171–179, doi:10.1098/rsta.1993.0085.

Pastre, J.-F., Singer, B.S., Guillou, H., Pupin, J.-P., and Riou, B., 2004, Chronostratigraphy of the key Upper Miocene (Lower Turolian) sequence of la Montagne d'Andance (Ardèche, France): Implications of new $^{40}Ar/^{39}Ar$ laser fusion and unspiked K-Ar dating of trachytic tephra and basalts: Bulletin de la Société Géologique de France, v. 175, p. 3–10, doi:10.2113/175.1.3.

Putnis, A., 2002, Mineral replacement reactions: From macroscopic observations to microscopic mechanisms: Mineralogical Magazine, v. 66, p. 689–708, doi:10.1180/0026461026650056.

Renard, F., and Ortoleva, P., 1997, Water films at grain-grain contacts: Debye-Hückel, osmotic model of stress, salinity, and mineralogy dependence: Geochimica et Cosmochimica Acta, v. 61, p. 1963–1970, doi:10.1016/S0016-7037(97)00036-7.

Renard, F., Dysthe, D.K., Feder, J., Bjørlykke, K., and Jamtveit, B., 2001, Enhanced pressure solution creep rates induced by clay particles: Experimental evidence in salt aggregates: Geophysical Research Letters, v. 28, p. 1295–1298, doi:10.1029/2000GL012394.

Robin, P., 1979, Theory of metamorphic segregation and related processes: Geochimica et Cosmochimica Acta, v. 43, p. 1587–1600, doi:10.1016/0016-7037(79)90179-0.

Rutter, E.H., 1976, The kinetics of rock deformation by pressure solution: Philosophical Transactions of the Royal Society of London A, v. 283, p. 203–219, doi:10.1098/rsta.1976.0079.

van Noort, R., Visser, H.J.M., and Spiers, C.J., 2008, Influence of grain boundary structure on dissolution controlled pressure solution and retarding effects of grain boundary healing: Journal of Geophysical Research, v. 113, B03201, doi:10.1029/2007JB005223.

Wheeler, J., 2014, Dramatic effects of stress on metamorphic rocks: Geology, v. 42, p. 647–650, doi:10.1130/G35718.1.

Wintsch, R.P., Aleinikoff, J.N., and Keewook, Y., 2005, Foliation development and reaction softening by dissolution and precipitation in the transformation of granodiorite to orthogneiss, Glastonbury Complex, Connecticut, USA: Canadian Mineralogist, v. 43, p. 327–347, doi:10.2113/gscanmin.43.1.327.

Manuscript received 17 February 2015
Revised manuscript received 29 July 2015
Manuscript accepted 30 July 2015

Printed in USA